TÜBİTAK

Turkish Journal of Medical Sciences

http://journals.tubitak.gov.tr/medical/

Research Article

Turk J Med Sci
(2013) 43: 379-387
© TÜBİTAK
doi:10.3906/sag-1204-85

The value of apparent diffusion coefficient measurements in the differential diagnosis of vertebral bone marrow lesions

Gülten TAŞKIN[1], Lütfi İNCESU[2], Kerim ASLAN[3,*]

[1]Department of Radiology Vezirköprü State Hospital, Samsun, Turkey
[2]Department of Radiology, Faculty of Medicine, Ondokuz Mayıs University, Samsun, Turkey
[3]Department of Radiology, Sinop Atatürk State Hospital, Sinop, Turkey

Received: 18.04.2012 • **Accepted:** 16.08.2012 • **Published Online:** 29.05.2013 • **Printed:** 21.06.2013

Aim: To be able to differentiate benign vertebral bone marrow lesions from malign lesions according to apparent diffusion coefficient (ADC) values, enabling quantitative assessment, and to determine the sensitivity and the specificity in differentiating benign and malign lesions according to the optimal cutoff ADC value.

Materials and methods: In 99 patients, 133 lesions in total were included in the study, 59 of which were benign (acute vertebral compression fracture depending on osteoporosis or trauma, spondylitis, atypical hemangioma), and 74 malign (malign compression fracture, metastasis). Each of the benign lesions was compared to the malign lesions. In the statistical analysis, normality tests, variance analysis tests, and the Tukey HSD multi-discriminant analysis tests were performed for all measurable variables. The optimal cutoff ADC value was determined by ROC analysis in the differentiation of benign and malignant lesions.

Results: The mean ADC value of the benign induced acute compression fractures was significantly higher than that of the malign induced compression fractures, and the mean ADC value of the spondylitis atypical hemangiomas was significantly higher than that of the malign lesions ($P < 0.0001$). According to the optimal cutoff value of 1.32×10^{-3} mm2/s, determined for the differentiation of benign and malignant vertebral bone-marrow lesions, sensitivity was 96.5%, specificity 95.2%, positive predictive value 96.5%, and negative predictive value 95.2%.

Conclusion: Vertebral bone-marrow pathologies were differentiated as benign or malignant with high sensitivity and specificity with the aid of ADC values calculated from maps obtained by DWI.

Key words: Vertebrae, diffusion-weighted MRI, apparent diffusion coefficient, atypical hemangioma

1. Introduction

Invasion of the fatty bone marrow by primary malignant tumors, metastatic malignancies, acute benign and malignant compression fractures, and infectious conditions cause similar signal changes in routine magnetic resonance imaging (MRI) studies (1,2). Although MRI has a high sensitivity in delineating the pathology, its specificity is low. For example, osteoporotic and metastatic compression fractures may be mistaken for each other in the acute phase. Edema in the acute phase of benign fractures may replace normal bone marrow and cause hypointense signal changes in T1-weighted images and hyperintense signal changes in T2-weighted images, at the same time taking contrast material. These changes are also typical for metastasis and cause confusion in diagnosis when only one lesion is present (3). It is quite important to determine whether a compression fracture has a malign or a benign cause, especially in patients with a primary malignancy. This is because compression fractures depending on osteopenia develop in these patients at a rate of one-third (4). Pyogenic bacteria, brucella, and tuberculosis infections are the most common causes of spondylodiscitis. Central nervous system tuberculosis, basal meningitis, hydrocephalus, edema, ischemia-infarct, abscess, and arachnoiditis may occur in various forms and may show different symptoms (5). Infections can sometimes be difficult to diagnose, especially when there is isolated vertebral body involvement without any soft tissue component, and adjacent disk involvement (6). Therefore, in order to plan appropriate therapy according to the precise diagnosis, the patients are exposed to invasive interventions such as biopsy (2,7,8).

* Correspondence: mdkerim@hotmail.com

Diffusion-weighted imaging (DWI) has recently appeared as a new method of screening in characterizing lesions without necessitating contrast material and in evaluating the vertebrae quantitatively (9,10). Currently, DWI obtained by single-shot echo-planar–spin-echo (SSEP-SE) T2 application of diffusion gradients is the best method for measuring in vivo the combined effects of capillary perfusion and diffusion by means of the apparent diffusion coefficient (ADC) (8). A loss of signals occurs as a result of the microscopic movements of the molecules in the diffusion-sensitivity sequences, and this loss is measured by calculating the ADC. The ADC depicts the specific diffusion capacity, microscopic structure, and organization of a biological tissue (9,11,12).

Some studies have been able to differentiate benign acute compression fractures from malign induced compression fractures according to ADC values (3,4,13–16). In a comparatively small number of surveys, ADC values have been studied in discriminating the infectious lesions from the malign lesions (4,5,17). Atypical hemangioma may have different appearances; it has a striated pattern in most cases and contains prominent vascular channels and an enlarged, prominent basivertebral venous plexus (18). However, it is important to differentiate atypical hemangiomas, which appear as hypointensity in T1A sequences and hyperintensity in T2A sequences, and which do not possess a striated pattern, from malign lesions with conventional MR sequences, especially in those with a primary malignancy from metastasis. Nevertheless, as far as we know, there is no study available in the literature performed using the DWI technique to differentiate atypical hemangiomas from malign lesions.

The purpose of this study was to differentiate acute benign compression fractures possessing benign vertebral marrow bone lesions, infection, and atypical hemangiomas from malign compression fractures, which are malign lesions, and metastasis according to the ADC value measurements, enabling quantitative assessment, and also to determine sensitivity and specificity in differentiating benign and malign lesions according to the optimal cutoff ADC value.

2. Materials and methods

2.1. Patients

The study group comprised 99 patients diagnosed with vertebral lesions during conventional vertebral colon MRI examination at Ondokuz Mayıs University, Medical Faculty Hospital, Radiology Department, between November 2009 and February 2011. The patients were aged 18–89 years (mean 54.99 ± 15.32). There were 51 females and 53 males; 133 vertebral lesions of a total of 99 patients were included in the study. The study protocol was approved by the ethics committee and the study was supported by the university research project. Consent was obtained from all the patients to participate in the study.

The vertebral lesions that were included in the study consisted of atypical hemangiomas, traumatic and osteoporotic acute benign compression fractures, spondylitis, metastases, multiple myeloma, and compression fractures due to malignant illnesses. In 32 patients, 44 acute vertebral compression fractures in total were detected. In 20 patients, there was a history of 27 fractures and traumas; they did not have a primary malignancy, there was no posterior element involvement on MRI, there was no epidural soft tissue mass, and conventional MR resulted in a benign compression fracture diagnosis depending on osteoporosis and trauma as a result of clinical follow-up. In 12 patients whose primary malignancy was proven histologically, of the 17 malign compression fractures (breast carcinoma in 3, lung carcinoma in 3, multiple myeloma in 2, prostatic carcinoma in 2, lymphoma in 1, synovial sarcoma in 1), 5 received a final diagnosis via biopsy, and 7 via bone scintigraphy, conventional MR sequences, and clinical follow-up.

In 16 spondylitis patients, 5 of which had a tuberculosis history, 23 infectious lesions in total were found. Of the 7 patients with 9 atypical hemangioma lesions, 1 had primary malignancy (stomach carcinoma). In 44 patients with primary malignancy (breast carcinoma in 7, lung carcinoma in 8, prostatic carcinoma in 3, lymphoma in 3, stomach carcinoma in 2, malign melanoma in 1, nasopharyngeal carcinoma in 1, thyroid carcinoma in 1, chondrosarcoma in one, endometrial cancer in 1, bladder carcinoma in 1, small bowel carcinoma in 1, testis carcinoma in 1, and multiple myeloma in 13), 57 metastatic lesions were found. Infectious spondylitis, atypical hemangiomas, and the final diagnosis of the metastasis were determined by computed tomography, bone scintigraphy, conventional MR sequences, typical clinical and laboratory findings, and clinical follow-up. Metastatic lesions in the patients with 17 primary malignancies received a histopathological diagnosis.

2.2. Magnetic resonance imaging

Conventional vertebral column MRI examinations were performed in all patients using a 1.5 Tesla MRI apparatus (Siemens Magnetom Symphony Quantum, Erlangen, Germany) with a spine coil. The routine sequences studied in patients with trauma consisted of T1-weighted spin echo (SE) and T2-weighted SE sagittal, T2-weighted SE axial, and short inversion time inversion recovery (STIR) sagittal sections, whereas in other patients routine sequences with contrast-enhanced T1-weighted SE sagittal and axial sections were investigated. All contrast-enhanced sequences were constructed over routine T1-weighted SE sequences, using the same parameters.

DWI was carried out before the contrast-enhanced sections. The sequences in DWI were obtained in the sagittal plane, using a finger pulse trigger from SSEP-SE T2. The b values were 0 and 500 s/mm^2. Technical parameters were as follows: TR/TE, 2500/94 ms; slice thickness, 5 mm; field of view, 450 mm; matrix, 80 × 128; bandwidth, 1396 Hz/pixel; NEX, 8; scanning duration, 2.37 s; gap, 0.5 mm; trigger pulse, 1.

2.3. Imaging analysis

DWI sequences were obtained by applying diffusion-sensitive gradients at different b values (0, 500 mm^2/s) in the sagittal plane in all 3 directions (x, y, z) to SSEP-SE T2. The 1st series consisted of EP-SE-T2 (b = 0, no diffusion gradient), and the 2nd series consisted of images with diffusion-sensitive gradients of b = 500 mm^2/s applied in the x, y, and z directions. Isotropic images were obtained by calculating the projection of diffusion vectors in 3 directions to every voxel for a b value of b = 500 mm^2/s. The isotropic images included images produced by the device, with the calculation of the cubic square root of the product of signal intensities measured in the x, y, and z directions, and the signal changes dependent on the direction were eliminated. The ADC map of isotropic images of b = 500 mm^2/s value was automatically produced by the device.

All DWI image clusters were transferred to a separate workstation for ADC measurements (Leonardo, software version 2.0; Siemens). ADC measurements were made on mean curve image analysis software, by ROI placed on every lesion on the ADC map created for a b value of b = 500 mm^2/s. The ROI were circular with diameters of 0.19–2.60 mm. Measurements were made in vertebrae with more than 3 lesions from the largest 3 lesions at most within the region with the least artifact. In lesions with a heterogeneous structure, measurements were made by DWI at the largest possible ROI of the brightest ADC images with the least signal.

2.4. Statistical analysis

All statistical analysis was carried out with the Statistical Package for the Social Sciences for Windows 15.0 (SPSS Inc., Chicago, USA). Normality tests were done for all measurable variables in the statistical analysis. All mean ADC values were compared and studied by one-way variance analysis for all subgroups (atypical hemangioma, acute benign compression fracture, spondylitis, metastasis, and malignant compression fracture). Comparisons for a difference in ADC values of lesion subgroups were conducted with the Tukey HSD and multiple difference tests. $P < 0.05$ was considered as the statistical significance level for all tests. The results are presented as the mean and the standard deviation, as well as the median, minimum, and maximum values.

The lesion area measurements were compared by nonparametric Kruskall–Wallis analysis of variance, as they did not show a normal distribution. Paired comparison of the groups was carried out with the Mann–Whitney U test, using Bonferroni correction. Spearman's rho coefficient was calculated to determine the relationship between ADC and area.

The optimal cutoff ADC value to separate the benign group (acute benign compression fracture, spondylitis, atypical hemangioma) from the malignant group (metastasis and malignant compression fracture) was determined by receiver operating characteristic (ROC) analysis. Sensitivity, specificity, and positive and negative predictive values were calculated according to this threshold value.

3. Results

A total of 99 patients found to have 133 vertebral bone marrow lesions were included in the study. The lesions were classified as benign or malignant, and the number of lesions in each group was 59 and 74, respectively. Of the benign lesions, 9 were atypical hemangiomas, 27 were acute benign (traumatic osteoporotic) compression fractures, and 23 were spondylitis, and of the malignant lesions, 57 were metastases and 17 were malign compression fractures.

Mean ADC values were calculated for every lesion group. The results are presented in the Table as the mean ± standard deviation, as well as the median, minimum, and maximum values (Table 1). ADC values for atypical

Table 1. Distribution of the measured mean ADC values in the lesions.

Lesion	Number	Mean ADC ± SD	Median (min–max)
Atypical hemangioma	9	1.80 ± 0.37	1.73 (1.94–2.82)
Acute benign compression fracture	27	1.75 ± 0.30	1.76 (1.29–2.28)
Spondylitis	23	1.54 ± 0.15	1.48 (1.34–1.86)
Metastasis	57	0.77 ± 0.30	0.78 (0.48–1.39)
Malignant compression fracture	17	0.94 ± 0.34	0.91 (0.43–1.44)

ADC = apparent diffusion coefficient (10^{-3} mm^2/s ± SD), SD = standard deviation, min = minimal, max = maximal

hemangiomas were 1.94–2.82 × 10^{-3} mm^2/s. The mean ADC value of the 9 atypical hemangiomas was 1.80 ± 0.37 × 10^{-3} mm^2/s (Figure 1). ADC values of acute benign compression fractures were 1.29–2.28 × 10^{-3} mm^2/s. The mean ADC value of the 27 benign compression fractures was 1.75 ± 0.30 × 10^{-3} mm^2/s. ADC values of spondylitis were 1.34–1.86 × 10^{-3} mm^2/s. The mean ADC value of the 23 spondylitis lesions was 1.54 ± 0.15 × 10^{-3} mm^2/s. ADC values of metastases were 0.48–1.39 × 10^{-3} mm^2/s, and the mean ADC value of the 57 metastatic lesions was 0.77 ± 0.30 × 10^{-3} mm^2/s (Figures 2 and 3). ADC values of compression fractures due to malignant causes were 0.43–1.44 × 10^{-3} mm^2/s. The mean ADC value of the 17 malign compression fractures was 0.94 ± 0.34 × 10^{-3} mm^2/s (Figure 4). The mean ADC values of the acute benign compression fractures were higher than those of the malignant compression fractures, and the mean ADC values of the spondylitis and atypical hemangiomas were higher than the mean ADC values of the malignant lesions, and this difference was statistically significant ($P < 0.0001$).

The lesions were grouped as benign (atypical hemangiomas and acute benign compression fractures, spondylitis) and malignant (metastases, malign compression fractures). The mean ADC values were calculated for these 2 groups, and the usefulness of ADC

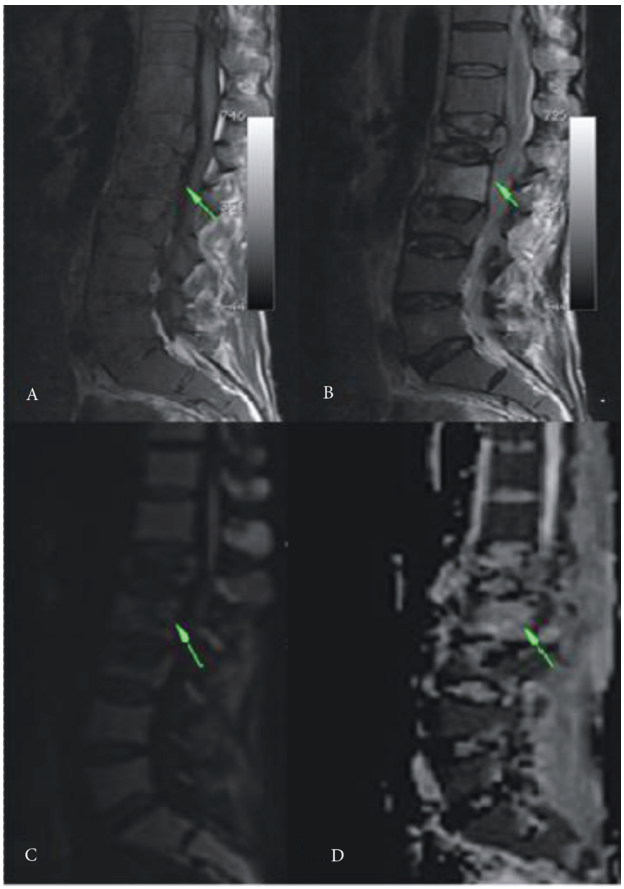

Figure 1. A–D. Atypical hemangioma of the spine (L2) in a male patient followed up for chronic lymphoid leukemia. The T1-weighted axial MR image (A) shows hypointensity in the round lesion with smooth contours (arrow). The T2-weighted axial MR image (B) shows hyperintensity in the lesion (arrow). DWI (C) shows hypointensities in these lesions due to increased diffusion (arrow). The ADC map (D) shows hyperintensity in the lesion (arrow). The mean ADC value is 2.82 × 10^{-3} mm^2/s at the ADC measurements of the lesion and supports a benign lesion. There are also benign compression fractures that do not show diffusion limitation at the L1 and L3 vertebrae.

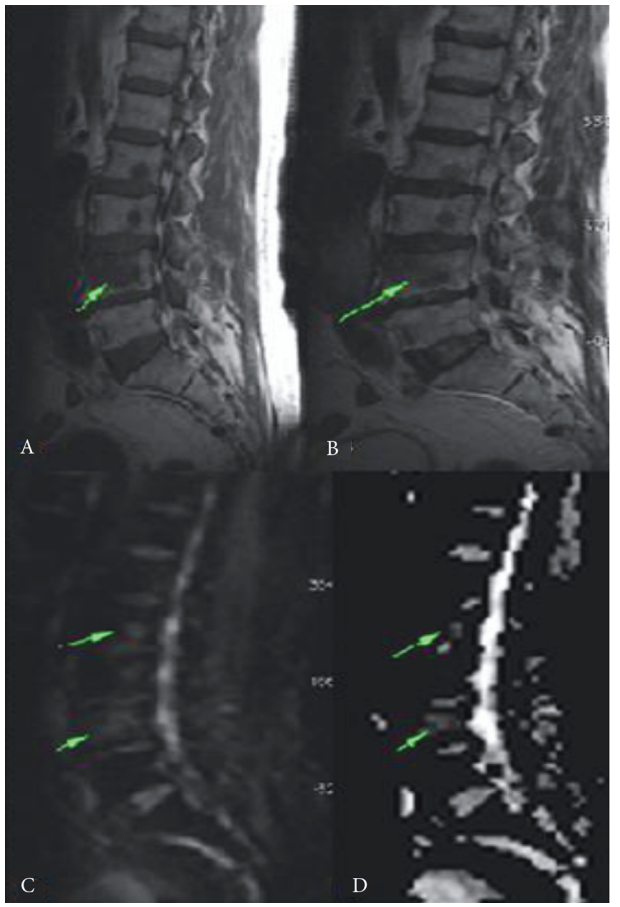

Figure 2. A–D. Widespread sclerotic metastases in the vertebrae of a 64-year-old patient with carcinoma of the prostate, the biggest one at the corpus of the L4 vertebra. The T1-weighted axial MR image (A) and T2-weighted axial MR image (B) show hypointensity in the lesions (arrow). DWI (C) shows hyperintensity in the lesions (arrows). The ADC map (D) shows hypointensities in these lesions due to restricted diffusion (arrows). The mean ADC value is 0.54 × 10^{-3} mm^2/s at the ADC measurement from the lesion at L4 vertebra, supporting metastasis.

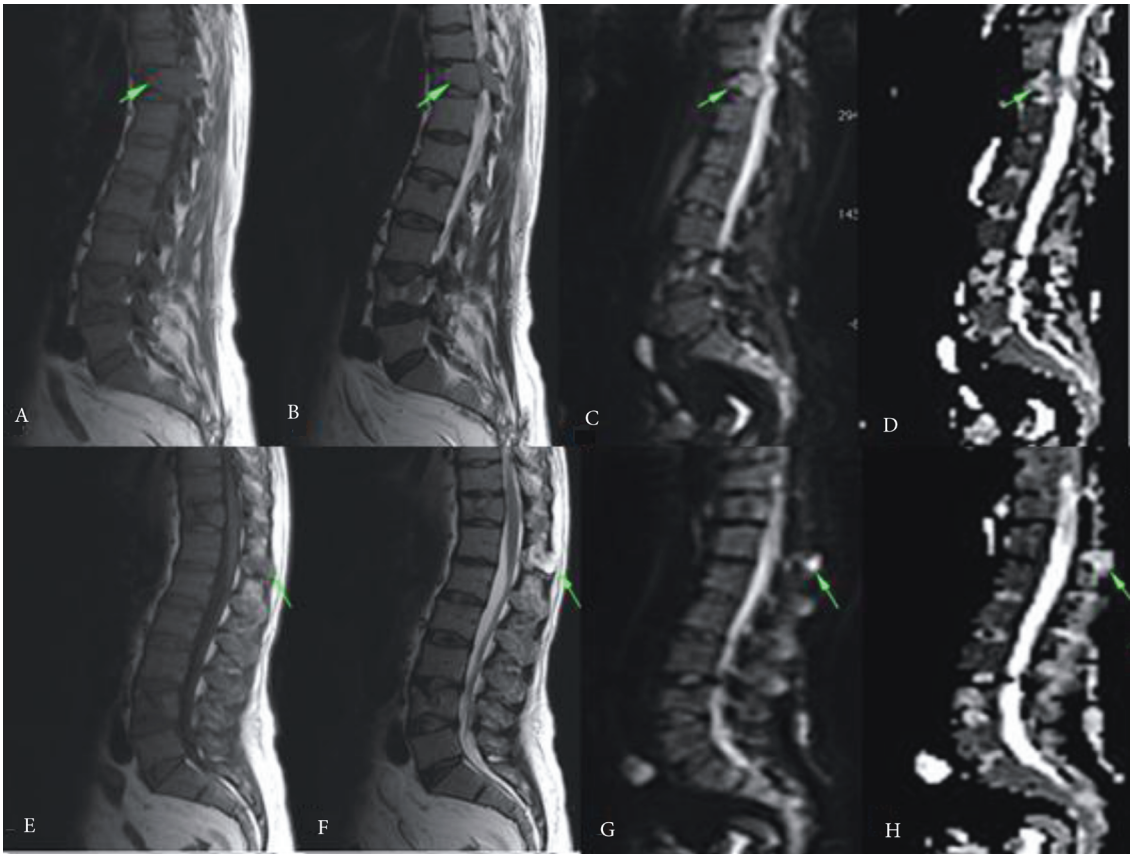

Figure 3. A–H. Active lesions at the T11 vertebra, and lesions that responded to treatment at the processus spinosus of the T12 vertebra of a 58-year-old patient being followed-up for multiple myeloma. The T1-weighted axial MR image (A) and T2-weighted axial MR image (B) show hypointensity in the round lesion with smooth contours at the T11 vertebra (arrow). DWI (C) shows hyperintensity in the lesions (arrow). The ADC map (D) shows hypointensities in these lesions due to restricted diffusion (arrow). The mean ADC value is 0.83×10^{-3} mm^2/s at the ADC measurement of the lesion and supports the involvement of multiple myeloma. There is a hypointense lesion at the processus spinosus of the T12 vertebra. The T1-weighted axial MR image (E) shows hypointensity in the round lesion (arrow). The T2-weighted axial MR image (F) shows hyperintensity in the lesion (arrow). DWI (G) and ADC maps (H) show hyperintensities in these lesions due to increased diffusion (arrow). DWI (G) shows hyperintensity in the lesion (arrow) due to T2 brightness. The mean ADC value is 2.41×10^{-3} mm^2/s at the ADC measurement of the lesion and supports response to treatment.

for differential diagnosis was investigated. The mean ADC value of benign lesions was found to be 1.66×10^{-3} mm^2/s ($1.29–2.82 \times 10^{-3}$ mm^2/s). The mean ADC value of malignant lesions was found to be 0.82×10^{-3} mm^2/s ($0.43–1.44 \times 10^{-3}$ mm^2/s) (Table 2). A statistically significant difference was detected in the comparison of the ADC values of these 2 groups ($P < 0.0001$). A threshold value was determined, using the ROC, in order to differentiate benign lesions from malignant ones. The threshold value for the mean ADC value was found to be 1.32×10^{-3} mm^2/s. Sensitivity, specificity, and positive and negative predictive values were calculated from this threshold value. When 1.32×10^{-3} mm^2/s was used as the threshold value, the mean ADC values of 3 of the 59 benign lesions were below it, and 3 of the 74 malignant lesions were above it (Table 3). According to the optimal threshold value of 1.32×10^{-3} mm^2/s set to differentiate vertebral bone marrow lesions as benign or malignant, sensitivity was found to be 96.5%, specificity 95.2%, positive predictive value 96.5%, and negative predictive value 95.2%.

The mean area of ROI that the measurements are made from was different for every lesion and did not show statistically normal distribution. Spearman's rho coefficient was calculated in order to investigate the relationship between the area of ROI for measurements and the mean ADC values. According to this calculation, $r = 0.20$, $P = 0.373$, and the relationship between them was not statistically significant.

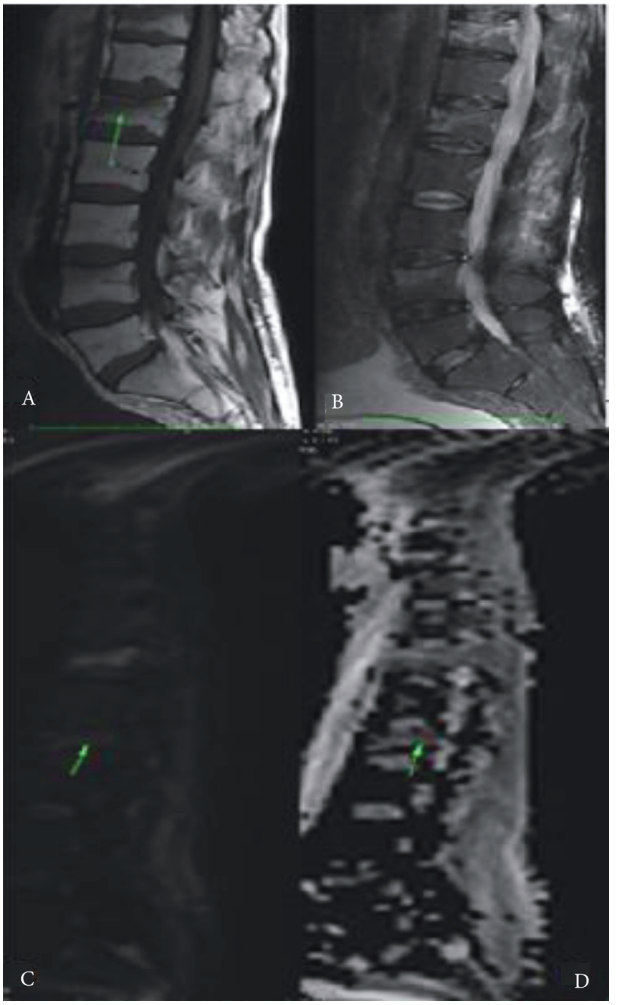

Figure 4. A–D. Malignant-appearing compression fractures, most prominent at the L1 vertebra of a 54-year-old patient without a known primary malignancy. The T1-weighted axial MR image (A) shows hypointensity in the lesion (arrow). The T2-weighted axial MR image (B) shows hyperintensity in the lesion (arrow). DWI (C) shows hyperintensity in the lesions (arrow). The ADC map (D) shows hypointensities in these lesions due to restricted diffusion (arrow). The mean ADC value is 0.81 $\times 10^{-3}$ mm^2/s from the ADC measurement of the lesion at L1, supporting a malignant pathology.

4. Discussion

DWI investigates the random microscopic movements of water molecules in the body, and the image contrast is dependent on the molecular movements of water. DWI has provided additional information relative to conventional sequences by reflecting the movements of water molecules in tissues, thus detecting even small changes in the microscopic structure of the tissues due to these movements (19). In tissues whose cellularity is increased, while diffusion limitation depending on the narrowing of the extracellular distance is displayed, free diffusion occurs in tissues whose cellularity is decreased and whose cell membrane is ruptured because of an extensive extracellular area. The movement of water molecules reveals a decrease in the measurement of signal intensity in DWI. The degree of movement of water molecules and the degree of signal loss have been found to be proportional (19,20). There are some important points to be considered in the evaluation of the spine with DWI. The parameters and type of sequence used are important, due to the complex anatomic structure and the presence of different physiological formations in the region studied. Artifacts are very few in the diffusion-weighted steady-state free precession (DW-SSFP) sequence, but it is not an appropriate technique for ADC measurements that enable quantitative assessment, because of complex signal occurrence (3,21). In our study, we used echo-planar sequences (EPI). The EPI sequence was a fast sequence, and it decreased the movement and susceptible artifacts, and, moreover, it presents the ADC measurements enabling quantitative assessment (4). It reflects tissue features such as ADC extracellular area width, viscosity, cell density, type, the shape of the fibers, and their closeness. When the movement of water molecules is restricted (for example, in tumors), ADC values decrease (20,22).

Baur et al. (23) used the DW-SSFP sequence first in the differentiation of 22 acute osteoporotic and/or traumatic fractures and 17 pathological vertebral compression fractures. They concluded that DW-SSFP enabled a perfect discrimination between pathological and benign vertebral compression fractures. In Abanoz et al. (21), there were 63 acute vertebral compression fractures due to trauma, osteoporosis, malignant tumor infiltration, or infection, and all traumatic or osteoporotic fractures were hypo- or iso-intense in appearance, and all malignant or infectious fractures were hyperintense. A statistically significant difference between fractures of traumatic or osteoporotic origin and malignant or infectious fractures was detected. Due to the fact that the signal in the DW-SSFP sequence used in this study depends on the T2 relaxation time, the high signal of the lesions is not only associated with the diffusion restriction dependent on the high cellularity of the neoplastic process. As the high signal is also dependent on the T2 signal (24) and it does not allow ADC measurements enabling quantitative assessment, we did not choose this sequence. In malignant vertebral fractures, fatty bone marrow is replaced by tumor cells, restricting the diffusion of free water molecules, and, accordingly, its ADC values are low. Benign acute vertebral fractures possess an increased amount of free water in the interstitial space, and they indicate increased water diffusion. Therefore, their ADC values are high. Our results support studies made by using quantitative ADC values in the

Table 2. Distribution of mean ADC values of benign, infectious, and malignant groups.

Group	Lesion number	Mean ADC ± SD	Median (min–max)
Benign	59	1.66 ± 0.33	1.64 (1.29–2.82)
Malignant	74	0.82 ± 0.30	0.81 (0.43–1.44)

SD = standard deviation, min = minimal, max = maximal, ADC = apparent diffusion coefficient

Table 3. Numeric distribution of lesions according to cut-off value of mean ADC ($1.32\ 10^{-3}$ mm^2/s).

Cutoff value for mean ADC	Number of malignant lesions	Number of benign lesions
1.32×10^{-3} mm^2/s or lower	71	3
Over 1.32×10^{-3} mm^2/s	3	56
Number of total lesions	74	59

ADC = apparent diffusion coefficient

literature (3,4,14–16,18,25). Furthermore, we found the mean ADC values of acute benign compression fractures to be statistically higher than those of malign compression fractures ($P < 0.0001$). In Wonglaksanapimon et al. (15), 7 malignant compression fractures and 32 benign compression fractures were evaluated. The discrepancy between the ADC values of the benign and malignant compression fractures was statistically significant ($P < 0.0001$). The results of our study are quite similar. Chan et al. (14) found no overlap between the ADC values of benign and malignant fractures, and detected a statistically significant difference between their ADC values. Our results are similar in that there is a significant difference between the ADC values of benign and malignant fractures and an absence of overlap.

In infectious lesions, the fact that there are no typical pre-/paravertebral abscess lesions or disk involvement makes the diagnosis difficult, and especially when it is found as a single vertebral lesion, its differentiation from malignant lesions may be difficult. In the literature, differentiation of infectious lesions and malignant lesions according to ADC values is not clear yet. Palle et al. (6) found the mean ADC values of 128 vertebral tuberculosis lesions in 56 patients to be 1.4×10^{-3} mm^2/s, and when they took this value as a cutoff in the discrimination of malignant lesions, they found 64.8% sensitivity, 75% specificity, and 74.5% positive predictive values. However, due to the fact that this ADC value displays values overlapping with the ADC values of metastatic vertebra lesions, they emphasized that the ADC values should be evaluated with the clinical history and routine MR findings. Pui et al. (17) found, respectively, sensitivity, specificity, and accuracy to be 60.26%, 66.00%, and 62.50% according to the 1.02×10^{-3} mm^2/s cutoff ADC values used in order to differentiate malignant lesions from infection. Balliu et al. (4) stated that the ADC values of infectious lesions and malignant lesions coincided, contrary to other studies, and therefore they could not differentiate them. In our study, the mean ADC values of infectious lesions were $1.54 \pm 0.15 \times 10^{-3}$ mm^2/s and were significantly higher than malignant lesions ($P < 0.0001$). Only 2 of the 23 vertebral infectious lesions displayed ADC values overlapping with malignant lesions, and the overlapping values were considerably few compared to the other studies. However, there is a need for a wider range in order to differentiate infectious lesions from malignant lesions according to their ADC values.

It may not be possible to differentiate atypical hemangiomas from malignant lesions if there is no hypointensity on conventional MR sequences, no hypointensity on T1A sequences, and no hyperintensity and striated patterns on T2A sequences. In patients known to have a primary malignancy, the lesion is usually single and located in the posterior of the corpus if peduncle involvement is accompanying, and its differential diagnosis is quite difficult. As far as we know, there is no research available in the literature attempting to differentiate atypical hemangiomas from malignant lesions according to the mean ADC values pursuant to the cutoff values. Leeds et al. (26) reported that hemangiomas may appear hypo- or hyperintense in DWI, but possess higher ADC

values than benign compression fractures or metastases. However, there is no information on ADC values for atypical hemangiomas. In our study, there were 9 atypical hemangioma lesions in 7 patients. In the patient with a chronic lymphoid leukemia, the lesion was posterior located, hypointense on T1A sequences, and hyperintense on T2A sequences, and it displayed a signal feature similar to metastasis. The ADC value of the lesion was 2.82×10^{-3} mm^2/s, obviously higher than the ADC values of metastases. It was shown that the lesion had a typical trabecular pattern for hemangioma on CT. There was no malign involvement on bone scintigraphy. No change was seen in the lesion in the follow-up, and an atypical hemangioma diagnosis was obtained. In our study, the mean ADC values of the atypical hemangiomas were 1.80×10^{-3} mm^2/s, and they displayed statistically significant differentiation from the malignant lesions ($P < 0.0001$). In no lesion was an overlap seen in ADC values. However, since the number of the atypical hemangioma was small in our study, studies of more extensive range are needed in order to confirm these findings.

Mean ADC values were calculated for the differentiation of malignant and benign lesions of the vertebral bone marrow, and these provided useful information for this discrimination. However, no cutoff value between these 2 groups has been calculated before. We were able to differentiate malign and benign lesions with a sensitivity of 96.5% and a specificity of 95.2%, with an optimal cutoff value of 1.32×10^{-3} mm^2/s.

As far as we know, there is no study investigating the relationship between the area used in the calculation of mean ADC value ROI and ADC values. According to our results, there are important differences in the mean ROI areas of lesions where measurements were made, and there is no statistically significant association between mean ADC value and area ($P > 0.05$).

In conclusion, malign and benign lesions of the vertebral bone marrow can be differentiated with high sensitivity and specificity using mean ADC values. In spite of the fact that it is possible to differentiate atypical hemangiomas from malign lesions according to the ADC values, the small number of patients is a limitation of our study. It should be supported by studies of more extensive range. According to the current study, there is no statistically significant association between the ROI used in the measurement of the lesion and the mean ADC value.

References

1. Moulopoulos LA, Yoshimitsu K, Johnston DA, Leeds NE, Libshitz HI. MR prediction of benign and malignant vertebral compression fractures. J Magn Reson Imaging 1996; 6: 667–74.
2. Herneth AM, Dominkus M, Kurtaran A, Lang S, Rand T, Kainberger F. Bone metastases: new trends in diagnostic imaging. Wien Med Wochenschr Suppl 2002; 113: 92–4.
3. Zhou XJ, Leeds NE, McKinnon GC, Kumar AJ. Characterization of benign and metastatic vertebral compression fractures with quantitative diffusion MR imaging. AJNR Am J Neuroradiol 2002; 23: 165–70.
4. Balliu E, Vilanova JC, Pelaez I, Puig J, Remollo S, Barcelo C et al. Diagnostic value of apparent diffusion coefficients to differentiate benign from malignant vertebral bone marrow lesions. European Journal of Radiology 2009; 69: 560–66.
5. Yaşar K, Pehlivanoğlu F, Şengöz A, Şengöz G. Evaluation of radiological findings in 160 adult patients with tuberculous meningitis. Turk J Med Sci 2012; 42: 259–67
6. Palle L, Reddy MB, Reddy KJ. Role of magnetic resonance diffusion imaging and apparent diffusion coefficient values in the evaluation of spinal tuberculosis in Indian patients. Indian J Radiol Imaging. 2010; 20: 279–83.
7. Frager D, Elkin C, Swerdlow M, Bloch S. Subacute osteoporotic compression fracture: misleading magnetic resonance appearance. Skeletal Radiol 1988; 17: 123–26.
8. Le Bihan D, Turner R, Douek P, Patronas N. Diffusion MR imaging: clinical applications. AJR Am J Roentgenol 1992; 159: 591–99.
9. Biffar A, Sourbron S, Dietrich O, Schmidt G, Ingrisch M, Reiser MF et al. Combined diffusion-weighted and dynamic contrast-enhanced imaging of patients with acute osteoporotic vertebral fractures. European Journal of Radiology 2010; 76: 298–303.
10. Bammer R, Fazekas F, Augustin M, Simbrunner J, Strasser FS, Seifert T et al. Diffussion-weighted MR imaging of the spinal cord. AJNR Am J Neuroradiol 2000; 21: 587–91.
11. Le Bihan D, Breton E, Lallemand D, Aubin ML, Vignaud J, Laval-Jeantet M. Separation of diffusion and perfusion in intravoxel incoherent motion MR imaging. Radiology 1988; 168: 497–505.
12. Herneth AM, Guccione S, Bednarski M. Apparent diffusion coefficient: a quantitative parameter for in vivo tumor characterization. Eur J Radiol 2003; 45: 208–13.
13. Spuentrup E, Buecker A, Adam G, van Vaals JJ, Guenther RW. Diffusion-weighted MR imaging for differentiation of benign fracture edema and tumor infiltration of the vertebral body. AJR Am J Roentgenol 2001; 176: 351–58.
14. Chan JH, Peh WC, Tsui EY, Chau LF, Cheung KK, Chan KB et al. Acute vertebral body compression fractures: discrimination between benign and malignant causes using apparent diffusion coefficients. Br J Radiol 2002; 75: 207–14.

15. Wonglaksanapimon S, Chawalparit O, Khumpunnip S, Tritrakarn SO, Chiewvit P, Charnchaowanish P. Vertebral body compression fracture: discriminating benign from malignant causes by diffusion-weighted MR imaging and apparent diffusion coefficient value. J Med Assoc Thai 2012; 95: 81–7.

16. Mubarak F, Akhtar W. Acute vertebral compression fracture: differentiation of malignant and benign causes by diffusion weighted magnetic resonance imaging. J Pak Med Assoc 2011; 61: 555–58.

17. Pui MH, Mitha A, Rae WI, Corr P. Diffusion-weighted magnetic resonance imaging of spinal infection and malinancy. J Neuroimaging 2005; 15: 164–70.

18. Raya JG, Dietrich O, Reiser MF, Baur-Melnyk A. Methods and applications of diffusion imaging of vertebral bone marrow. J Magn Reson Imaging 2006; 24: 1207–20.

19. Koh DM, Collins DJ. Diffusion-weighted MRI in the body: applications and challenges in oncology. AJR Am J Roentgenol 2007; 188: 1622–35.

20. Bammer R. Basic principles of diffusion-weighted imaging. Eur J Radiol 2000; 345: 169–84.

21. Abanoz R, Hakyemez B, Parlak M. Diffusion vertebral imaging of acute vertebral compression fractures: differential diagnosis of benign versus malignant pathologic fractures. Tani Girisim Radyol. 2003; 9: 176–83.

22. Thoeny HC, De Keyzer F. Extracranial applications of diffusion-weighted magnetic resonance imaging. Eur J Radiol 2007; 17: 1385–93.

23. Baur A, Stäbler A, Bruning R, Bartl R, Krödel A, Reiser M et al. Diffusion-weighted MR imaging of bone marrow: differentiation of benign versus pathologic compression fractures. Radiology 1998; 207: 349–56.

24. Castillo M, Arbelaez A, Smith JK, Fisher LL. Diffusion-weighted MR imaging offers no advantage over routine noncontrast MR imaging in the detection of vertebral metastases. AJNR Am J Neuroradiol 2000; 21: 948–53.

25. Tang G, Liu Y, Li W, Yao J, Li B, Li P. Optimization of b value in diffusion-weighted MRI for the differential diagnosis of benign and malignant vertebral fractures. Skeletal Radiol 2007; 36: 1035–41.

26. Leeds NE, Kumar AJ, Zhou XJ, McKinnon GC. Magnetic resonance imaging of benign spinal lesions simulating metastasis: role of diffusion-weighted imaging. Top Magn Reson Imaging 2000; 11: 224–34.